INTERNATIONAL JOURNAL OF AGRICULTURE & BIOLOGY
ISSN Print: 1560–8530; ISSN Online: 1814–9596
20F–105/2020/24–6–1479–1486
DOI: 10.17957/IJAB/15.1586
http://www.fspublishers.org

Full Length Article

Transcriptome Profiling Reveals Association of the Regulatory Pathways of Yellow Leaf Color Mutant with Chlorophyll Synthesis and Photosynthesis in Sesame (*Sesamum indicum*)

Tongmei Gao[1], Xinyong Pei[2], Xiaoyu Su[1], Libin Wei[1], Chun Li[1], Feng Li[1], Yuan Tian[1], Dongyong Wang[1] and Shuangling Wei[1*]

[1]*Henan Sesame Research Center, Henan Academy of Agricultural Sciences/ Key Laboratory of Oil Crops in Huanghuai Hai Plains, Zhengzhou, Henan 450002, China*

[2]*Agricultural Economy & Information Research Institute, Henan Academy of Agricultural Sciences, Zhengzhou, Henan 450002, China*

[*]For correspondence: wsl041162@126.com

Received 05 June 2020; *Accepted* 13 July 2020; *Published*_____

Abstract

For green plants, variations in the leaf color, which are closely related to chlorophyll metabolism and photosynthesis, can reduce photosynthetic capacity and efficiency. However, the regulatory mechanism of leaf color formation, especially for sesame, is still not clear. Leaf color mutants are an ideal material to explore regulatory pathways associated with chlorophyll synthesis and photosynthesis. In this study, the green (*yy* type) and the yellow (*YY t*ype) leaf color progenies of the sesame mutant (*Siyl-1*) were compared by RNA sequencing and physiological analysis. Physiologically, the yellow colored mutant leaves had lower chlorophyll content and almost no photochemical conversion efficiency. Of the 540 differentially expressed genes (DEGs) identified, 320 were up-regulated and 220 down-regulated. Of these, 7 DEGs were involved in chlorophyll biosynthesis (*CAO*), photosynthesis (*Lhca2*, *Lhcb3*, and *Lhcb6*) and carbon fixation in photosynthetic organisms (*ALDO*, *PckA*, and *rpiA*). The expression of these genes, except *ALDO* and *rpiA*, was significantly suppressed in the yellow leaf color mutant. Moreover, the DEGs included transcription factor and heat shock protein genes that might be important for the regulation of gene expression in the aspect of chlorophyll synthesis and chloroplast development. Thus, results might provide a more integrated picture about the regulatory mechanism of leaf color formation for sesame. © 2020 Friends Science Publishers

Keywords: Sesame (*Sesamum indicum* L.); Leaf color mutant; Transcriptome; Chlorophyll biosynthesis; Transcription factor

Introduction

In higher plants, leaf color mutation is a common phenomenon in nature and has received widespread attention from both researchers and the general public because of the obvious features and ease of distinguishing different leaf colors (Li *et al.* 2018). There are numerous leaf color mutants that have been stratified into different categories (Gustafsson 1942) such as albino, xantha, viridis, virescent and zebra; these variations in leaf color are attributed to the loss of balance between the biosynthesis and degradation of pigments in plants (Wu *et al.* 2018). Mechanism of yellow formation, which are generally closely related to chlorophyll biosynthesis and chloroplast development, have been investigated in various crop varieties (Petersen *et al.* 2004; Schippers *et al.* 2008; Sang *et al.* 2010; Guan *et al.* 2016) such as *Arabidopsis*, maize, wheat, rice and barley.

Chlorophyll is an important photosynthetic pigment in plants; it is embedded in the antenna protein complexes and is responsible for the absorption of light energy and its transmission and transduction to the chloroplasts (Tanaka and Tanaka 2006). Chlorophyll synthesis is regulated by more than 15 enzymes and 20 genes (Nagata *et al.* 2005). A decrease in the expression levels of these genes could inhibit synthesis of chlorophyll (Adhikari *et al.* 2011; Li *et al.* 2016), leading to reduced chlorophyll content and variation in leaf color in higher plants (Rebeiz 2014). For the rice (*ygl-1*) mutant with yellow-green leaf, the expression of *CAO* and *cab1R* genes encoding the light-harvesting chlorophyll-protein complex (LHC) family proteins were severely suppressed, leading to the blockage of chlorophyll biosynthesis and chloroplast development (Xu *et al.* 2006; Wu *et al.* 2007). In *Lagerstroemia indica*, the yellow leaf color mutation induced the expression of genes involved in chlorophyll degradation and suppressed the genes

expression of chlorophyll biosynthesis (Li *et al.* 2015b). In addition, in wheat, genes related to photosynthesis and carbon fixation were found to be responsible for the changes in leaf coloration (Wu *et al.* 2018). Thus, several reports have confirmed that chlorophyll biosynthesis and chloroplast development are affected in leaf color mutants.

Sesame (*Sesamum indicum* L.), as an oil seed crop, referred as the "queen of oil seed crops" (Anilakumar *et al.* 2010). Previously, it had been reported that yellow-green leaf color sesame mutant (*Siyl-1)* provides an ideal germplasm to understand the mechanisms of chlorophyll metabolism, photosynthesis, and chloroplast development (Gao *et al.* 2019). Thus far, few studies have focused on sesame leaf color mutants. Our previous studies on the sesame leaf color mutant only focused on phenotypic traits, physiological and biochemical characteristics, and genetic analysis. However, the underlying regulatory mechanism on leaf color mutation for sesame remains poorly understood.

In this study, the phenotypic traits of sesame with normal green leaves (*yy*) and mutant yellow leaves (*YY*) were compared and analyzed for physiological, biochemical characteristics and transcriptome profile. Several DEGs involved in chlorophyll synthesis, photosynthesis and carbon fixation, as well as encoding transcription factor (TF) family members were identified and responsible for the regulation of the expression of genes related to photosynthesis and pigment synthesis. These results could form the basis to understand the complex metabolic networks for yellow leaf color mutation in sesame.

Materials and Methods

Plant materials

The sesame yellow-green leaf mutant (*Siyl-1*) was produced from the sesame cultivar yuzhi 11 with a common leaf color by ethyl methane sulfonate (EMS) mutagenesis. In our previous study, the *Siyl-1* mutation in sesame was determined to be controlled by an incompletely dominant nuclear gene, which produced three leaf color phenotypes (yellow-green leaf (*Yy*), yellow leaf (*YY*) and normal green leaf (*yy*)) upon selfing (Gao *et al.* 2019). The cotyledons of the three leaf color phenotypes were used for physiological experiments. The yellow leaf (*YY*) and normal green leaf (*yy*) were sampled for RNA-seq and quantitative real-time PCR (qRT-PCR). All collected samples were rapidly frozen in liquid nitrogen before stored in a cryogenic refrigerator (−80°C). Three replicates were performed for each sample.

Analysis of chlorophyll fluorescence parameters

The chlorophyll fluorescence parameters [Fv/Fm, photochemical efficiency of PSII; ETR (II), electron transport rate of PSII] were measured using a two-channel modulated chlorophyll fluorescence analyzer (Dual-PAM-100; Zealquest Scientific Technology Co., Ltd., Shanghai, China). After the plants were acclimated to the dark for 30 min, the initial fluorescence (F_0) and maximum fluorescence (F_m) were measured, and chlorophyll fluorescence parameters were measured according to manufacturer instructions. The fluorescence parameters were calculated using a built-in analysis software of the chlorophyll fluorescence analyzer (Dual-PAM, v. 1.18).

RNA extraction, library preparation, and RNA-seq

The cDNA libraries were constructed using 6 samples with normal green leaves (*yy*) and yellow leaves (*YY*) designated as *yy*-1, -2, -3 and *YY*-1, -2, -3. For each sample, Total RNA extraction was performed by a plant RNA extraction kit (TaKaRa, Dalian, China), following its instructions. The concentration of RNA was confirmed using the NanoDrop 2000 (Thermo, Wilmington, D.E., U.S.A.). The RNA integrity was performed by the Agilent Bioanalyzer 2100 system (Agilent Technologies, C.A., U.S.A.). The library of cDNA was constructed and sequenced by Biomarker Technologies Co., Ltd. (Beijing, China).

Sequence alignment and functional annotation

Data were processed by eliminating adapter sequences and ploy-N-containing and low-quality reads from the raw data. The clean reads were aligned with the sesame reference genome sequences available on NCBI. The following databases were used for functional annotation, including: Nr, NCBI non-redundant protein sequence database; Pfam protein family database; KOG/COG, Clusters of Orthologous Groups of protein database; Swiss-Prot, a manually annotated and reviewed protein sequence database; KO, KEGG Ortholog database; GO, Gene Ontology.

DEG analysis

The expression levels of genes were assessed according to FPKM by cuffquant and cuffnorm software software (Li *et al.* 2015b). The FDR (false discovery rate) < 0.05 and $|\log_2$ (fold change) $| \geqslant 1$ was defined as significant DEGs.

GO analysis of the DEGs was performed by the GO seq R packages (Young *et al.* 2010). KOBAS software was used to analyzed the statistical enrichment of the DEGs in the KEGG pathways (Mao *et al.* 2005).

Verification of gene expression by qRT-PCR

The accuracy of the RNA-seq data was validated by randomly selecting several leaves color-related DEGs. All specific primers of DEGs were designed with Primer Premier 5.0 software (Table S1). The cDNA was synthesized using a PrimerScript™ RT reagent kit (TaKaRa, Dalian, China). The qRT-PCR analysis was conducted according to manufacturer's instructions using a SYBR Premix Ex TaqTM II Kit (TaKaRa, Dalian, China)

equipped with a QuantStudio® 7 Flex Real-Time PCR system (Applied Biosystems, Shanghai, China). The results were normalized using the *SiTUB* gene as an endogenous standard (Wei *et al.* 2013). Expression level of the genes was analyzed using the $2^{-\Delta\Delta Ct}$ method (Livak and Schmittgen 2001). All analyses were performed three times for all biological replicates.

Statistical analysis

Data analysis was performed by one-way analysis of variance, and figures were plotted using GraphPad Prism 5 (GraphPad Software, U.S.A.). All data are presented as the means ± standard deviation (SD, n = 3). The least significant difference test was used to test significance.

Results

Changes in phenotypic characterization and physiological parameters in mutant leaves

Three phenotypes—normal green (*YY*), yellow-green (*Yy*), and yellow (*yy*) types—were obtained by the segregation of the yellow-green leaf color mutant (*Yy)* in a self-pollinated progeny (Fig. 1A). The *yy* type has similar agronomic traits as those of the wild type (WT, Yuzhi 11), and type *Yy* was also not different from the WT except for the variation in leaf color. Interestingly, the *YY* type was extremely yellow and rapidly died after germination. No significant change in chlorophyll fluorescence parameters was noted for normal green (*yy*) and WT. However, compared with those of the normal green (*yy*) type, the Fv/Fm and ETR (II) of the *Yy* type were reduced by 55.7 and 36.6%, respectively. The chlorophyll fluorescence parameters were extremely reduced for the *YY* type (Fig. 1B, C).

RNA-Seq analysis

The potential molecular basis for color formation in the yellow leaf color mutant was further understood using the cotyledon of the *YY* and *yy* types to construct cDNA libraries using the Illumina HiSeqTM X10 platform (Illumina, San Diego, C.A., U.S.A.). After removing low-quality reads, a total of 35.97 Gb clean data was obtained (Table 1). For each sample, 5 GB or above clean data were obtained. The clean paired end reads ranged from 21,368,657 to 22,261,358 for the *YY* type and from 17,048,612 to 19,701,252 for the *yy* type. For each sample, the GC content varied from 48.80 to 49.62%, and the Q30 base was 93.03% or above. Clean reads of each sample were sequentially aligned with the sesame reference genome, with the efficiency ranging from 94.81 to 95.84%. The correlation values between the replicates of the samples ranged from 0.97 to 0. 99 (Fig. S1). 92.54% or above clean reads were mapped to the exon region of the genome (Table S2), confirming that the sequencing quality was reliable for subsequent analysis.

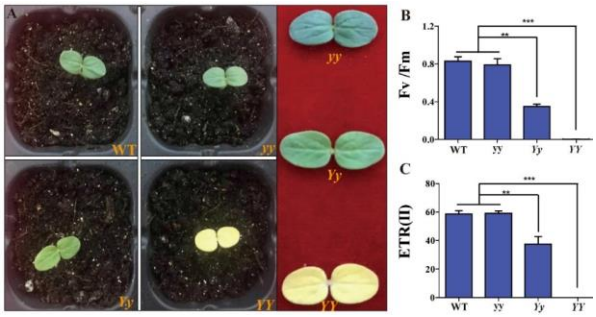

Fig. 1: Measurements of phenotypic and physiological indices in *YY*, *Yy*, and *yy* progeny of sesame leaf color mutant (Siyl^{-1}) and Yuzhi 11 (WT). (**A)** Phenotypes of the progeny of *Siyl-1* and Yuzhi 11 (WT). (**B**) Measurements of Fv/Fm for the WT and progeny of *Siyl-1*. (**C)** Measurements of ETR (II) for the WT and progeny of *Siyl-1*. Two (**) and three asterisks (***) were used to indicate significant ($P < 0.01$) and extremely significant ($P < 0.001$) differences, respectively. *YY*, yellow leaf color in the progeny of *Siyl-1*; *Yy*, yellow-green leaf color in the progeny of *Siyl-1*; *yy*, normal green leaf color in the progeny of *Siyl-1*; WT, Yuzhi 11

Overview of DEGs between the *yy* and *YY* types

In all, 15,261 and 15,368 genes were quantitated, respectively, from *yy* and *YY* leaves (Fig. 2A). The DEGs were identified between *yy* and *YY* types, and 540 DEGs were identified, of which 320 and 220 were up- and down-regulated, respectively (Fig. 2B, C). Hierarchical clustering revealed significantly different DEG expression between the *yy* and *YY* types (Fig. 2D).

Annotated analysis of DEGs

The DEGs functions were annotated according to the GO database by the Blast2GO software suite. For biological process, the 540 DEGs were principally enriched in metabolic process, cellular process, and single-organism process. For cellular component, the DEGs were enriched in cell part and organelle. For molecular function, the DEGs were enriched in catalytic activity, binding, and transporter activity (Fig. S2). In addition, the DEGs were analyzed and assigned to 71 KEGG pathways, some of which are shown in Fig. 3A. Further enrichment analysis revealed the DEGs associated with protein processing in ER and photosynthesis-antenna proteins (Fig. 3B).

DEGs regulating chlorophyll metabolism and photosynthesis are involved in yellow leaf color formation

The key DEGs involved in the yellow leaf color formation were further investigated by identifying some DEGs related to chlorophyll metabolism and photosynthesis by the KEGG pathways analysis (Fig. 4). One DEG (*CAO*) in the

Table 1: Descriptive statistics of the transcriptome sequencing data for the yellow leaves of *YY* types and green leaves of *yy* types in sesame

Samples	Clean reads [i]	Clean bases [ii]	GC Content [iii]	% ≥ Q30 [iv]	Mapped Reads [v]
yy-1	22,261,358	6,656,006,414	48.80%	93.91%	41,180,208 (95.46%)
yy-2	21,368,657	6,386,365,320	49.10%	94.03%	42,670,653 (95.84%)
yy-3	21,569,434	6,454,682,306	49.11%	93.61%	40,805,506 (95.48%)
YY-1	18,339,669	5,483,145,836	49.62%	93.76%	37,513,493 (95.21%)
YY-2	19,701,252	5,884,235,364	49.33%	93.03%	34,774,099 (94.81%)
YY-3	17,048,612	5,100,971,244	49.12%	93.63%	32,587,834 (95.57%)

[i]Clean reads: Amount of pair-end reads in clean data;
[ii]Clean bases: The total number of bases in clean data;
[iii]GC content: The percentage of two bases (G and C) of the total base in clean data;
[iv]Q30%: The percentage of bases with a mass value greater than or equal to 30 in clean data;
[v]Mapped Reads: The number of reads to the reference genome and the percentage of clean reads

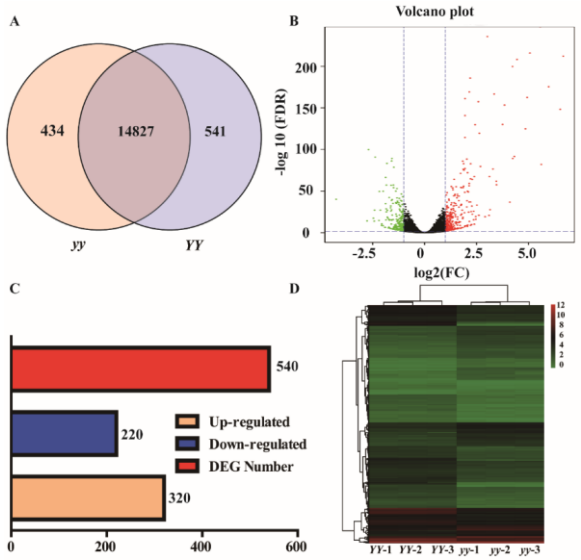

Fig. 2: Overview of transcriptome data obtained from *YY* and *yy* types. **(A)** Venn diagrams of genes identified in *YY* and *yy* types. The numbers of specific genes and shared genes be counted if one or more of the three replicates in each sample is quantified. **(B)** the volcano plots comparing gene expression between *YY* and *yy* types. **(C)** Number of differentially expressed genes (DEGs). **(D)** Heat map of the hierarchical cluster for DEGs

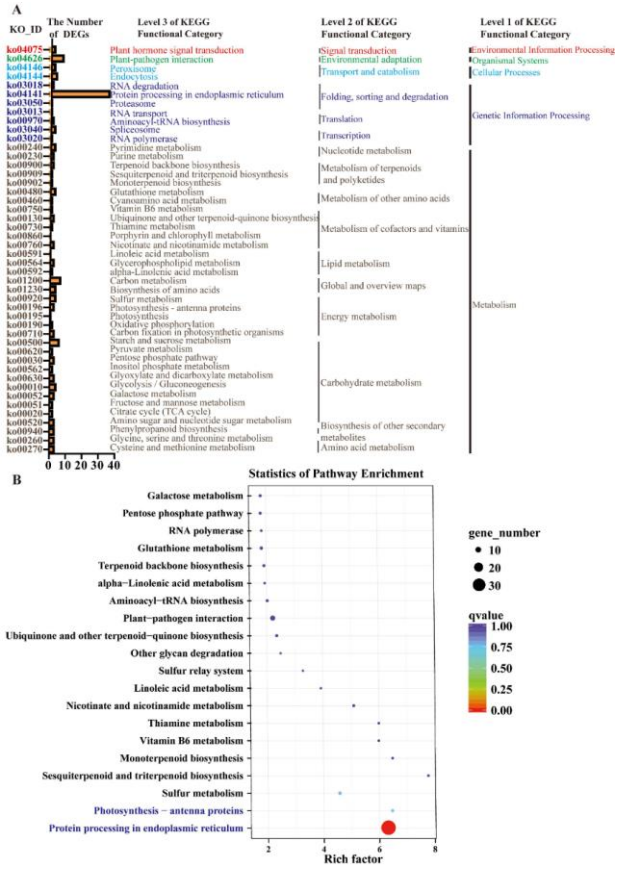

Fig. 3: KEGG pathway analysis of DEGs between *YY* and *yy* types. a KEGG classification analysis of DEGs between *YY* and *yy* types. b Pathway enrichment analysis of DEGs

chlorophyll synthesis pathway was down-regulated in the mutant *YY* type compared to the normal green leaf (*yy*) type. Moreover, the expression levels of three DEGs, *i.e.*, *Lhca2*, *Lhcb3*, and *Lhcb6*, in the LHC family associated with photosynthesis-antenna proteins were significantly down-regulated in the mutant. Moreover, three DEGs associated with carbon fixation in photosynthetic organisms were identified. Among them, two DEGs (*ALDO* and *TKTA)*—were up-regulated in the mutant *YY* type, whereas t*RpiA* was down-regulated.

DEGs encoding TF and heat shock proteins in the mutant *YY* type

TFs play important roles to activate or repress gene expression. In all, 99 TFs were found among the 25 DEGs identified in the mutant *YY* type; these were further divided into 13 TF families. The majority of the TFs were members of the AP2/ERF family (16%), followed by the C2C2 family (16%), MYB family (16%), GRAS family (8%), C2H2 family (8%), and NAC family (8%; Fig. 5A, Table S3). Four TFs of the AP2/ERF family were up-regulated, and four DEGs associated with C2C2 TFs were down-regulated in the mutant *YY* type. The expression levels of the TFs associated with MYB, GRAS, and C2H2 family are

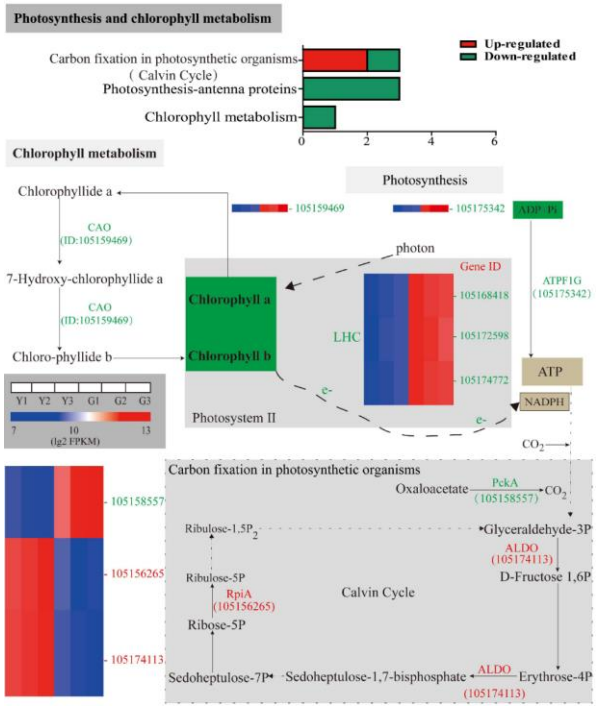

Fig. 4: Differences in the expression profiles of DEGs involved in chlorophyll metabolism and photosynthesis between *YY* and *yy* types in sesame

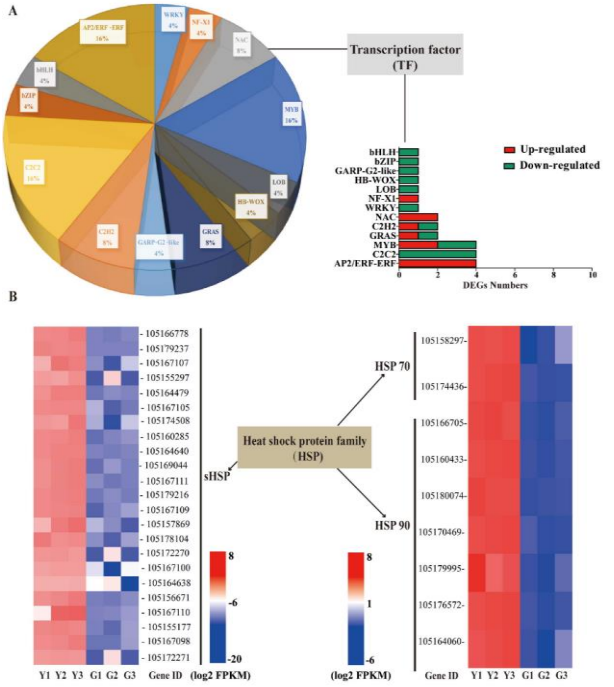

Fig. 5: Differences in the expression profiles of DEGs associated with transcription factors (TFs) and heat shock proteins (HSPs) between *YY* and *yy* types. **(A)** Analysis of DEGs encoding TFs. **(B)** Expression profiles of DEGs associated with HSPs

shown in Table S3. Moreover, a total of 32 heat shock proteins (HSPs) were identified in the DEGs of the mutant *YY* type, of which 23, 2, and 7 were associated with sHSP, HSP70, and HSP90 family members, respectively, and showed higher expression in the *YY* type (Fig. 5B).

Validation of RNA-seq data by qRT-PCR

The accuracy of the RNA-seq result was verified by quantifying the expression levels of 10 identified DEGs related to chlorophyll metabolism, TFs, HSPs, and photosynthesis using qRT-PCR analysis (Fig. 6). Among these DEGs mentioned above, 3 genes were associated with TF families and 3 with HSPs; 1 gene (*CAO*) was involved in chlorophyll metabolism; and 3 genes (*ALDO*, *TKTA*, and *RpiA*) were involved in photosynthesis. The expression pattern of these 10 DEGs detected using qRT-PCR was found to be the same as that revealed by the RNA-seq data. In general, the expression trend of the selected genes by qRT-PCR was in line with that of RNA-seq except for the difference in the expression level, indicating the reliability of the RNA-seq data.

Discussion

The measurements of chlorophyll contents and chloroplast ultrastructure revealed that the chlorophyll *a* and *b* contents of the *Yy* and *YY* types were significantly lower than green

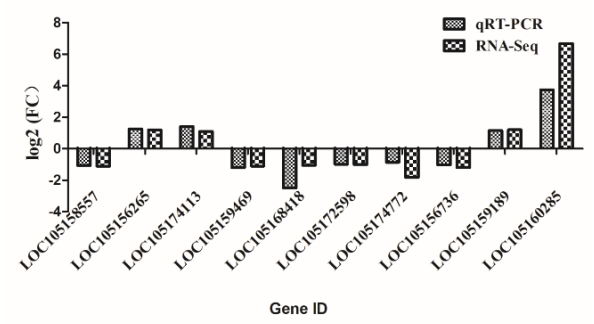

Fig. 6: Quantitative real-time PCR validation of the 10 DEGs selected from the RNA-seq data

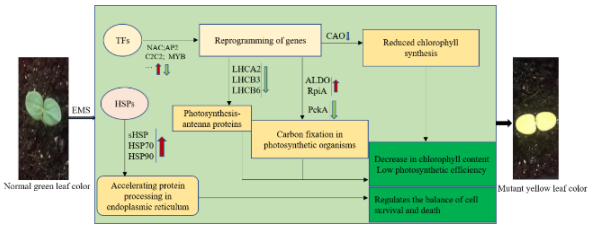

Fig. 7: A potential mode pathway of yellow leaf color formation in the *YY* type mutant. The arrows marked in red and green indicate upregulated and downregulated DEGs, respectively

leaves (*yy*), and the chloroplast structure varied evidently (Gao *et al.* 2019). The chlorophyll fluorescence measurements showed that the Fv/Fm and ETR (II) of the

Yy and *YY* types showed similar variations as those in chlorophyll contents, unlike in the normal green leaf (*yy*) type. These results showed that the leaf color mutations in sesame are most likely related to chlorophyll synthesis and photosynthesis. The critical regulatory pathways of leaf color mutation in the yellow-green leaf sesame mutant *Siyl-1* were further explored by analyzing the transcriptomes of the normal green (*yy*) and yellow (*YY*) types by RNA-seq. Several DEGs involved in Chl biosynthesis, photosynthesis, and TFs were identified in the mutant *YY* type.

The balance of chlorophyll content in plants depends on chlorophyll synthesis and degradation (Tanaka and Tanaka 2006). Some studies have shown that the chlorophyll deficient mutant was mainly formed owing to the lack of enzymes in the chlorophyll synthesis process (Wu *et al.* 2007; Li *et al.* 2015a; Zhao *et al.* 2016). In present study, the expression of the *CAO* gene (LOC105159469) was significantly downregulated in the yellow (*YY*) types; this gene encodes chlorophyllide, a oxygenase that catalyzes the conversion of chlorophyll *a* to chlorophyll *b*. The *CAO* gene is essential for the regulation of chlorophyll biosynthesis and maintenance of photosynthetic antenna size (Sakuraba *et al.* 2007). The absence of *CAO* gene results in declined chlorophyll content and deficient phenotypes. In *Arabidopsis thaliana*, the *ch1-1* mutant containing a deletion of the *CAO* gene exhibited phenotypic characteristics of chlorosis and showed photodamage (Yamasato *et al.* 2005). In addition, in rice, the mutant of *pgl* gene encoding chlorophyllide an oxygenase 1 induced chlorophyll degradation, disorderly arrangement of chloroplast, reactive oxygen species accumulation, and leaf premature senescence (Yang *et al.* 2015b). Moreover, the over-expression of *OsCAO1* can induce chlorophyll *b* accumulation and inhibit leaf senescence in plants (Sakuraba *et al.* 2012). The present study physiological and biochemical results further support this conclusion. This evidence indicates that the *CAO* gene plays important roles in chlorophyll biosynthesis to regulate leaf color formation.

The chloroplast comprises the membrane, thylakoid, and matrix; among them, the thylakoid membrane is the key site for light absorption and energy transfer (Mirkovic *et al.* 2016). Photosynthesis proceeds methodically owing to the multi-subunit pigment–protein complexes embedded in the thylakoid membranes. The complexes consist mainly of PSII, PSI, light-harvesting complexes, cytochrome b6/f, and ATP synthase (Dekker and Boekema 2005). More studies have shown that color formation of leaf is closely associated with chloroplast development (Yu *et al.* 2007; Yang *et al.* 2015a). The previous studies on chloroplast structure showed that the formation of yellow leaf color was affected by impaired chloroplast. In plant leaves, LHCs mainly consist of chlorophyll and apoproteins required for assembling chlorophyll, which play an important role in the transfer of the captured light energy to the photosynthetic reaction center (Jansson 1994). Decrease in LHC levels has been known to cause changes in the size of photosynthetic antenna and induce photodamage. In a chlorina mutant of *A. thaliana*, the expression of the *LHC* gene was significantly suppressed, or even completely absent, resulting in the disorganization of grana stacking in the chloroplast (Kim *et al.* 2009). In this study, three DEGs (*Lhca2*, *Lhcb3*, and *Lhcb6*) identified are associated with the LHC gene family, and these genes were downregulated in the *YY* type mutant. Furthermore, the expression of one DEG (*ATPF1G*) encoding F-type H^+-transporting ATPase subunit gamma involved in ATP synthesis was inhibited in the mutant, and, of the three DEGs associated with carbon fixation in photosynthetic organisms, one was downregulated (*pckA*) encoding phosphoenolpyruvate carboxykinase (ATP) and two were upregulated (*ALDO* and *rpiA*) encoding fructose-bisphosphate aldolase, class I and ribose 5-phosphate isomerase A, respectively. The qRT-PCR results further confirmed the accuracy of the data. In the wheat yellow leaf color mutants, several DEGs were also identified, such as *PsaC*, *PsbB*, and *ATPase*, which significantly downregulated compared to those in the normal green color type, leading to reduced photosynthetic capacity (Wu *et al.* 2018). Along with the reduction of chlorophyll fluorescence parameters, the changes in the gene expression levels showed that the DEGs involved in photosynthesis affected the structure of chloroplasts and reduced photosynthetic rate and decreased chlorophyll content, resulting in the yellow phenotype formation.

TFs regulate the gene expression by binding to various specific DNA elements upstream of target genes, thereby activating or inhibiting the transcriptional activity of target genes and regulating their spatiotemporal specific expression (Riechmann and Ratcliffe 2000; Yamasaki *et al.* 2013). Many studies have shown that TFs are involved in the regulation of the expression of genes related to photosynthesis and chlorophyll metabolism, which lead to the variations in plant leaf color. The photosensitive pigment interaction factor *PIFs* belong to the basic helix-loop-helix TF family can regulate the development of chloroplast and content of chlorophyll (Huq *et al.* 2004). The arcuate nucleus TF family can interact with the *FtsZ* gene, regulate chloroplast division, and affect chlorophyll content (Maple and Møller 2006). *SlNAP2* belongs to the NAC TF family and can activate *SlSAG113* gene associated with chlorophyll degradation to promote leaf senescence in tomato (Huq *et al.* 2004). The AP2/ERF family members were induced by abiotic stress and involved in plant stress response (Xing *et al.* 2017). In present study, 25 TF family members identified, includes AP2/ERF, C2C2, MYB, and GRAS and these TFs may influence leaf coloration. Similarly, DEGs associated with AP2-EREBP, MYB, and C2H2 family TFs were identified in *Ginkgo biloba* with golden leaf coloration (Li *et al.* 2018). Many WRKY family and C2C2 TFs were enriched in the wheat mutant *(m68)* with a premature leaf senescence characteristic (Zhang *et al.* 2018). These results suggest that TFs can regulate gene

expression associated with chlorophyll synthesis to affect it and cause a change in leaf color.

Moreover, 32 DEGs annotated to the HSP family were found to be related to protein processing in ER. Interestingly, all these genes were upregulated in the mutant. HSPs are known to play vital roles in stress resistance processes. Numerous HSP-encoding genes were induced to express during abiotic stress to repair damaged proteins. Therefore, it is speculated that HSPs act as a stress response regulator and were induced to avoid excessive photosynthetic damage and maintain cell homeostasis in the mutant *YY* type.

Conclusion

The results showed that lower chlorophyll contents and almost no photochemical conversion efficiency in the yellow colored mutant leaves. Gene expression differed considerably between the green (*yy*) and the mutant yellow (*YY*) leaves, according to the transcriptional sequence analysis. Many DEGs and TFs were involved in chlorophyll synthesis and photosynthesis, were identified. Changes in gene expression led to less chlorophyll content, abnormal structure of chloroplasts, and reduced photochemical efficiency, which might have been closely related to the formation of yellow leaf color mutant. Overall, a rough outline was formed to speculate the possible regulation mechanism for the formation of yellow leaf phenotype in sesame (Fig. 7). The findings might help explain the mechanism of yellow color leaf formation in sesame and facilitate the improvement of selective breeding for leaf color varieties.

Acknowledgements

This research is supported by the China Agriculture Research System (CARS-14-1-14).

Author Contributions

All authors conceived the research. TG, XP and DW performed the experiments. FL, DW and YT prepared all plant materials. TG and XS analysis all data with the help of LW and CL. TG and SW wrote the manuscript, LW and XP revised it. All authors read and approved the final manuscript.

References

Adhikari ND, JE Froehlich, DD Strand, SM Buck, DM Kramer, RM Larkin (2011). GUN4-porphyrin complexes bind the ChlH/GUN5 subunit of Mg-Chelatase and promote chlorophyll biosynthesis in *Arabidopsis*. *Plant Cell* 23:1449–1467

Anilakumar KR, A Pal, F Khanum, AS Bawa (2010). Nutritional, medicinal and industrial uses of sesame (*Sesamum indicum* L.) seeds-an overview. *Agric Conspect Sci* 75:159–168

Dekker JP, EJ Boekema (2005). Supramolecular organization of thylakoid membrane proteins in green plants. *Biochim Biophy Acta Bioener* 1706:12–39

Gao TM, SL Wei, J Chen, Y Wu, F Li, LB Wei, C Li, YJ Zeng, Y Tian, DY Wang, HY Zhang (2019). Cytological, genetic, and proteomic analysis of a sesame (*Sesamum indicum* L.) mutant *Siyl-1* with yellow-green leaf color. *Genes Genomics* 42:25–39

Guan H, X Xu, C He, C Liu, Q Liu, R Dong, T Liu, L Wang (2016). Fine mapping and candidate gene analysis of the leaf-color gene *ygl-1* in maize. *PLoS One* 11; Article e0153962

Gustafsson ÃK (1942). The plastid development in various types of chlorophyll mutations. *Hereditas* 28:483–492

Huq E, B Al-Sady, M Hudson, C Kim, K Apel, P Quail (2004). Phytochrome-interacting factor 1 is a critical bHLH regulator of chlorophyll biosynthesis. *Science* 305:1937–1941

Jansson S (1994). The light-harvesting chlorophyll ab-binding proteins. *Biochim Biophys Acta Bioener* 1184:1–19

Kim EH, XP Li, R Razeghifard, JM Anderson, KK Niyogi, BJ Pogson, WS Chow (2009). The multiple roles of light-harvesting chlorophyll a/b-protein complexes define structure and optimize function of Arabidopsis chloroplasts: A study using two chlorophyll b-less mutants. *Biochim Biophys Acta Bioener* 1787:973–984

Li C, Y Hu, R Huang, XZ Ma, Y Wang, TT Liao, P Zhong, FL Xiao, CH Sun, ZJ Xu, XJ Deng, PR Wang (2015a). Mutation of FdC2 gene encoding a ferredoxin-like protein with C-terminal extension causes yellow-green leaf phenotype in rice. *Plant Sci* 238:127–134

Li Y, Z Zhang, ZY Zhang, P Wang, SA Wang, LL Ma, LF Li, RT Yang, YZ Ma, Q Wang (2015b). Comprehensive transcriptome analysis discovers novel candidate genes related to leaf color in a *Lagerstroemia indica* yellow leaf mutant. *Genes Genomics* 37:851–863

Li W, S Tang, S Zhang, JG Shan, CJ Tang, QN Chen, GQ Jia, YH Han, H Zhi, XM Diao (2016). Gene mapping and functional analysis of the novel leaf color gene *SiYGL1* in foxtail millet [*Setaria italica* (L.) P. Beauv]. *Physiol Plantarum* 157:24–37

Li WX, SB Yang, ZG Lu, ZC He, YL Ye, BB Zhao, L Wang, B Jin (2018). Cytological, physiological, and transcriptomic analyses of golden leaf coloration in *Ginkgo biloba* L. *Hortic Res* 5:12–26

Livak KJ, TD Schmittgen (2001). Analysis of relative gene expression data using real-time quantitative PCR and the $2^{-\Delta\Delta CT}$ method. *Methods*25:402–408

Mao X, T Cai, JG Olyarchuk, LP Wei (2005). Automated genome annotation and pathway identification using the KEGG Orthology (KO) as a controlled vocabulary. *Bioinformatics* 21:3787–3793

Maple J, SG Møller (2006). Plastid division: Evolution, mechanism and complexity. *Ann Bot* 99:565–579

Mirkovic T, EE Ostroumov, JM Anna, RV Grondelle, Govindjee, GD Scholes (2016). Light absorption and energy transfer in the antenna complexes of photosynthetic organisms. *Chem Rev* 117:249–293

Nagata N, R Tanaka, S Satoh, A Tanaka (2005). Identification of a vinyl reductase gene for chlorophyll synthesis in *Arabidopsis thaliana* and implications for the evolution of *Prochlorococcus* species. *Plant Cell* 17:233–240

Petersen BL, MG Møller, PE Jensen, KW Henningsen (2004). Identification of the Xan-g Gene and Expression of the Mg-chelatase Encoding Genes Xan-f,-g and-h in Mutant and Wild Type Barley (*Hordeum Vulgare* L.). *Hereditas* 131:165–170

Rebeiz CA (2014). Some major steps in the understanding of the chemistry and biochemistry of Chl. *In: Chlorophyll Biosynthesis and Technological Application*, pp:1–32. Springer, The Netherlands

Riechmann JL, OJ Ratcliffe (2000). A genomic perspective on plant transcription factors. *Curr Opin Plant Biol* 3:423–434

Sakuraba Y, S Balazadeh, R Tanaka, B Mueller-Roeber, A Tanaka (2012). Overproduction of Chl b retards senescence through transcriptional reprogramming in *Arabidopsis*. *Plant Cell Physiol* 53:505–517

Sakuraba Y, A Yamasato, R Tanaka, B Mueller-Roeber, A Tanaka (2007). Functional analysis of N-terminal domains of *Arabidopsis* chlorophyllide a oxygenase. *Plant Physiol Biochem* 45:740–749

Sang XC, LK Fang, YY Vanichpakorn, YH Ling, P Du, FM Zhao, ZL Yang, GH He (2010). Physiological character and molecular mapping of leaf-color mutantwyv1in rice (*Oryza sativa* L.). *Genes Genomics* 32:123–128

Schippers JHM, A Nunes-Nesi, R Apetrei, J Hille, AR Fernie, PP Dijkwel (2008). The *Arabidopsis* onset of leaf death mutation of quinolinate synthase affects nicotinamide adenine dinucleotide biosynthesis and causes early ageing. *Plant Cell* 20:2909–2925

Tanaka A, R Tanaka (2006). Chlorophyll metabolism. *Curr Opin Plant Biol* 9:248–255

Wei LB, HM Miao, RH Zhao, XH Han, TD Zhang, HY Zhang (2013). Identification and testing of reference genes for sesame gene expression analysis by quantitative real-time PCR. *Planta* 237:873–889

Wu HY, NR Shi, XY An, C Liu, HF Fu, L Cao, Y Feng, DJ Sun, LL Zhang (2018). Candidate genes for yellow leaf color in common wheat (*Triticum aestivum* L.) and major related metabolic pathways according to transcriptome profiling. *Intl J Mol Sci* 19:1594–1620

Wu ZM, X Zhang, B He, LP Diao, SL Sheng, JL Wang, XP Guo, N Su, LF Wang, L Jiang, CM Wang, HQ Zhai, JM Wan (2007). A chlorophyll-deficient rice mutant with impaired chlorophyllide esterification in chlorophyll biosynthesis. *Plant Physiol* 145:29–40

Xing L, Z Di, W Yang, J Liu, M Li, X Wang, C Cui, X Wang, X Wang, R Zhang, J Xiao, A Cao (2017). Overexpression of *ERF1-V* from *Haynaldia villosa* can enhance the resistance of wheat to powdery mildew and increase the tolerance to salt and drought stresses. *Front Plant Sci* 8; Article 1948

Xu PZ, Y Li, S Yuan, HY Zhang, H Peng, HH Lin, XD Wang, XJ Wu (2006). Studies of photosystem complexes and chlorophyll synthesis in chlorophyll-deficient rice mutant W1. *Sci Agric Sin* 39:1299–1305

Yamasaki K, T Kigawa, M Seki, K Shinozaki, S Yokoyama (2013). DNA-binding domains of plant-specific transcription factors: Structure, function, and evolution. *Trends Plant Sci* 18:267–276

Yamasato A, N Nagata, R Tanaka, A Tanaka (2005). The N-terminal domain of chlorophyllide a oxygenase confers protein instability in response to chlorophyll b accumulation in *Arabidopsis*. *Plant Cell* 17:1585–1597

Yang Y, X Chen, B Xu, Y Li, Y Ma, G Wang (2015a). Phenotype and transcriptome analysis reveals chloroplast development and pigment biosynthesis together influenced the leaf color formation in mutants of *Anthurium andraeanum* 'Sonate'. *Front Plant Sci* 6; Article 139

Yang YL, J Xu, LC Huang, YJ Leng, LP Dai, YC Rao, L Chen, YQ Wang, ZJ Tu, J Hu, DY Ren, GH Zhang, L Zhu, LB Guo, Q Qian, D Zeng (2015b). PGL, encoding chlorophyllide a oxygenase 1, impacts leaf senescence and indirectly affects grain yield and quality in rice. *J Exp Bot* 67:1297–1310

Young MD, MJ Wakefield, GK Smyth, A Oshlack (2010). Gene ontology analysis for RNA-seq: Accounting for selection bias. *Genome Biol* 11; Article R14

Yu F, A Fu, M Aluru, S Park, Y Xu, HY Liu, XY Liu, A Foudree, M Nambogga, S Rodermel (2007). Variegation mutants and mechanisms of chloroplast biogenesis. *Plant Cell Environ* 30:350–365

Zhang Q, C Xia, LC Zhang, CH Dong, X Liu, XY Kong (2018). Transcriptome analysis of a premature leaf senescence mutant of common wheat (*Triticum aestivum* L.). *Intl J Mol Sci* 19:782–800

Zhao SL, WH Long, YH Wang, LL Liu, YL Wang, M Niu, M Zheng, D Wang, JM Wan (2016). A rice White-stripe leaf3 (wsl3) mutant lacking an HD domain-containing protein affects chlorophyll biosynthesis and chloroplast development. *J Plant Biol* 59:282–292